EPJ Photovoltaics **14**, 34 (2023)

https://doi.org/10.1051/epjpv/2023028

Available online at:
www.epj-pv.org

Special Issue on 'EU PVSEC 2023: State of the Art and Developments in Photovoltaics', edited by Robert Kenny and João Serra

REGULAR ARTICLE

OPEN ACCESS

Experimental evaluation of the impact of pigment-based colored interlayers on the temperature of BIPV modules

Markus Babin*, Ingvar Haukur Jóhannsson, Michael Linde Jakobsen, and Sune Thorsteinsson

DTU Electro, Frederiksborgvej 399, 4000 Roskilde, Denmark

Received: 30 June 2023 / Received in final form: 15 September 2023 / Accepted: 10 October 2023

Abstract. While colored photovoltaics are gaining popularity in the market for building-integrated photovoltaics (BIPV), several specific properties are not accounted for in standard PV performance models. This work shows how relying on the coloration efficiency alone can lead to significant errors regarding module temperatures. By comparing measured temperature data from a test installation featuring BIPV façade elements in multiple colors, little correlation is found between total optical losses (reflection and absorption losses) and module temperature. Instead, better correlation is found with total reflectance. This is attributed to the light absorbed in the pigment-based colored layers contributing to module heating, whereas reflected light does not. This is especially relevant for colors with high lightness, such as gray or beige, for which reflection losses are dominating absorption losses. When modelling colored BIPV products, it is therefore recommended to only consider reflection losses for the irradiance contributing to module heating, while continuing to also include absorption losses for the effective irradiance used in electrical performance modelling.

Keywords: BIPV / colored PV / temperature modelling / performance modelling

1 Introduction

In recent years, colored PV has gained in popularity, with an increase in both manufacturers and different coloring technologies present on the market. This is mainly driven by interest in building-integrated photovoltaics (BIPV), where coloration is a vital factor in achieving pleasing aesthetics.

Several studies have investigated performance of different colored BIPV products − however most of them focused purely on the performance at standard test conditions (STC). The optical losses, both absorption and reflection losses, are still the dominating loss factors in most colored BIPV products, therefore their reduction is one of the main goals in developing new products and improving existing ones.

Theoretical studies have shown that, in the absence of absorption losses and considering idealized reflectance spectra, most colors could be reproduced with losses below 10 % [1]. It has also been shown that the theoretical efficiency limits are most affected by color lightness, with hue and saturation playing a lesser role. Light, neutral colors like gray generally show high losses, as light is reflected over larger portions of the visible spectrum [2].

PV performance models consist of a number of submodels, ranging from models for irradiance transposition, shading and spectral mismatch, to models for cell temperature, IV-performance and DC-AC conversion. In a typical modelling process, specific submodels are used to determine an effective irradiance, which is then used as an input to the subsequent submodels [3]. This effectively disconnects optical losses (both reflection and absorption losses), which are typically used to determine the effective irradiance, and thermal models for calculating module and cell temperature.

One of the major error source when modelling performance of PV installations is the module temperature estimation based on irradiance. This is especially true for building-integrated photovoltaics (BIPV) due to reduced ventilation, which in many cases lead to higher average operating temperatures. The effects of mounting configuration have been studied extensively, as well as different models suitable for simulating BIPV temperatures and performance. One such model is the Ross temperature model, which correlates PV module temperature with irradiance, and has been shown to be suitable for BIPV façade and rain screen installations [4,5].

An additional factor for the higher operating temperature of BIPV is the increasingly common use of glass-glass modules for both structural stability and reduced flammability, as opposed to standard glass-backsheet

* e-mail: marbab@dtu.dk

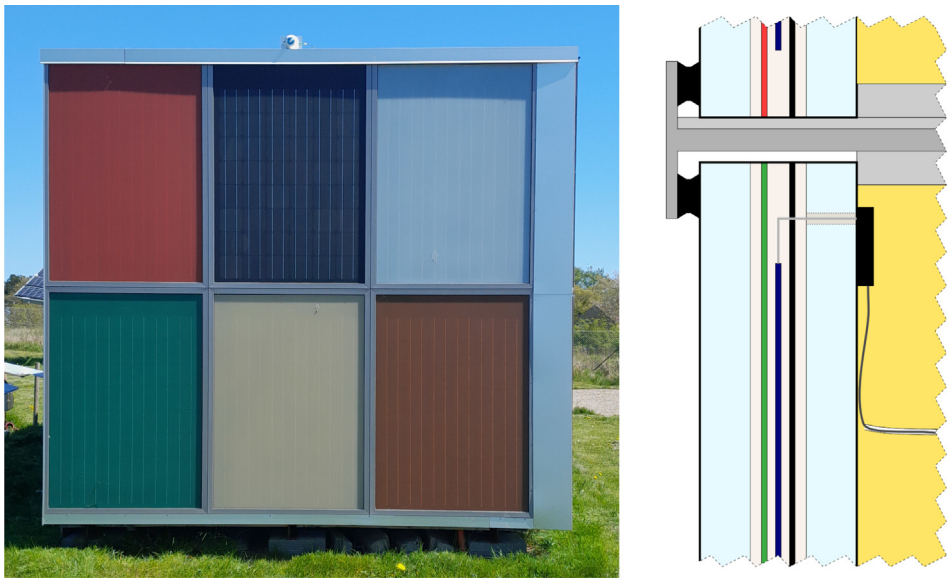

Fig. 1. West façade of the BIPV test site (left) and cross-sectional drawing of module and mounting structure (right).

modules. This leads to a higher thermal capacitance, due to the increased mass of glass covers compared to backsheets, as well as a larger thermal resistance between cell and module backside [6–8]. In combination with higher temperatures due to reduced ventilation, this can lead to longer periods at elevated temperatures, which may lead to accelerated degradation of materials in BIPV modules. This is partially offset by non-optimal system orientations and tilts, leading to reduced irradiance.

In a previous study, one shortcoming of common models in predicting the effective irradiance from colored BIPV has been shown, specifically that the choice of colorant has an impact on angular-dependent optical losses [9]. However, module and cell temperature modelling of colored BIPV modules has received little attention in scientific literature. Therefore, this work aims to identify any obvious issues specific to temperature modelling of colored BIPV.

2 Methodology

2.1 Outdoor test site

A BIPV façade test site was constructed at DTU Risø campus in Spring 2022 in order to investigate performance and temperature of BIPV modules under operating conditions. It consists of a retrofitted office container, where the south, west and east façades have been replaced with BIPV elements. The six elements on the west façades feature five different colors as well as an uncolored BIPV reference (top center), as shown in Figure 1. The five different colors include three saturated, dark colors (red, green and terracotta) as well as two lighter colors (gray and beige). The figure also shows a cross-sectional drawing of the module composition and mounting structure.

Each of the modules consists of 48 cells (2-busbar, Al-BSF, ~17 % efficiency) connected in series and laminated under 4 mm satinated glass using a UV-blocking polyolefin elastomer (POE) encapsulant. The colored modules each also contain a pigmented polymeric interlayer between two layers of encapsulant in front of the cell strings. The rear side of all modules contain a black interlayer as well as a 4 mm rear glass, and thus each colored module contains a total of 4 layers of encapsulant.

Modules are mounted directly in contact with the mineral wool insulation in the prefabricated façades elements using rubber gaskets to prevent moisture ingress through the side of the glass-glass laminates. DC cables from the module junction boxes are routed through the insulation to the inside of the container, where they are interconnected.

In order to operate each module at its maximum power point (MPP), they are outfitted with Huawei SUN2000P-375W power optimizers, connected to a Huawei SUN2000-2-KTL-L1 inverter. Electrical data (both input and output) from the optimizers is reported through inverter communication in 5 min intervals. In addition, each module is equipped with a Class A Pt100 temperature sensor mounted centrally on the module backside. Irradiance in plane of array (G_{POA}) is monitored using an EKO MS-80S-E pyranometer mounted on the top of the façades. Both temperature and irradiance data are reported in 10 s intervals.

Located next to the BIPV façade test site, a south-facing coupon test stand was constructed in Autumn 2022 to further investigate the thermal balance of BIPV modules, as can be seen in Figure 2. It features six single-cell coupons with similar composition to the façade-mounted modules, however only three different colors are present in this installation, as well as two reference samples

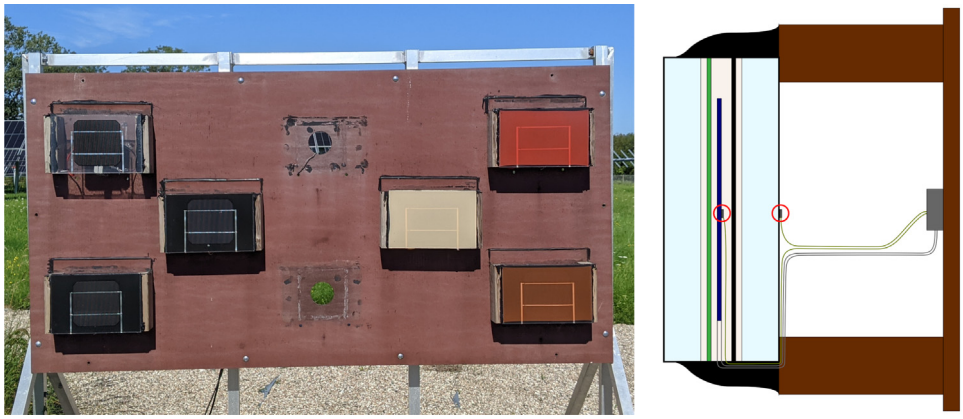

Fig. 2. South-facing coupon test stand (left) and cross-sectional drawing of coupons, mounting structure and highlighted temperature sensors (right).

and one sample without the black interlayer material. Another difference compared to the façade-mounted system is the use of standard PV glass for both front and back side instead of satinated glass. In addition, thermocouples are integrated directly in the samples to allow measurements of the cell temperature in addition to the back-of-module temperature measurements, highlighted in Figure 2 [10]. The modules are mounted on vertical lumber beams, allowing for free vertical airflow behind them. Each of the mini-modules is connected to a shunt resistor, which allows them to continuously operate in short-circuit conditions. Cell and back-of-module temperature as well as short-circuit current are measured in 10 s intervals.

In addition to the already stated parameters, the components of solar irradiance as well as ambient air temperature and wind are measured at a weather station approximately 250 m from the test site.

2.2 Data treatment and analysis

In the present analysis, performance and temperature data from the BIPV façade is included in the period of August 19, 2022 to June 10, 2023, and for the coupon test site starting from March 28, 2023 up to June 10, 2023. As a first step, data from the outdoor test site is filtered for data outside of realistic ranges, e.g., ambient temperatures below −20 °C, or above 50 °C, to capture measurement artifacts and errors. Subsequently, timestep mismatch between the data sources is eliminated by linear interpolation and resampling to common 10 s timesteps.

The Ross temperature coefficients for the models are determined by plotting the temperature difference ΔT between back-of-module and ambient against the in-plane irradiance G_{POA}. To compare the temperature difference between modules, the relative module temperature difference ΔT_{rel} for a colored module compared to the reference is calculated using equation (1). Here, T_a refers to the measured ambient air temperature, while $T(color)$ and $T(ref)$ refer to the measured module or cell temperatures of the samples and reference, respectively.

$$\Delta T_{rel}(color) = \frac{\Delta T(color)}{\Delta T(ref)} = \frac{T(color) - T_a}{T(ref) - T_a}. \quad (1)$$

Plotting this relative temperature difference against the in-plane irradiance G_{POA} allows for direct comparison of the reduction in module heating through reflection in the colored layers. Excluding nighttime and intermittently cloudy periods by limiting G_{POA} to $\geq 200\,\mathrm{W/m^2}$ allows for linear fitting of the relative temperature difference over irradiance to determine a relative Ross coefficient.

2.3 Laboratory measurements

In addition to the outdoor measurements, IV-curves of both the façade-mounted modules and single-cell coupons are measured at STC to determine the optical losses caused by the colored interlayers. They are calculated according to equation (2) as the I_{sc} ratio between each colored and the reference module.

$$\tau_{rel}(color) = \frac{I_{sc}(color)}{I_{sc}(ref)}. \quad (2)$$

Furthermore, total reflection spectra of the colored mini-modules are measured using an integrating sphere, a collimated beam from an Energetic EQ-99 X laser-driven light source and an Ocean Optics QE65000 spectrometer, following a measurement procedure described previously [9].

3 Results

As an initial overview, Figure 3 shows the temperature difference between measured back-of-module temperature and ambient temperature for the six façade-integrated modules on a clear-sky day. For one, the figure clearly shows the delayed heating and cooling response of the

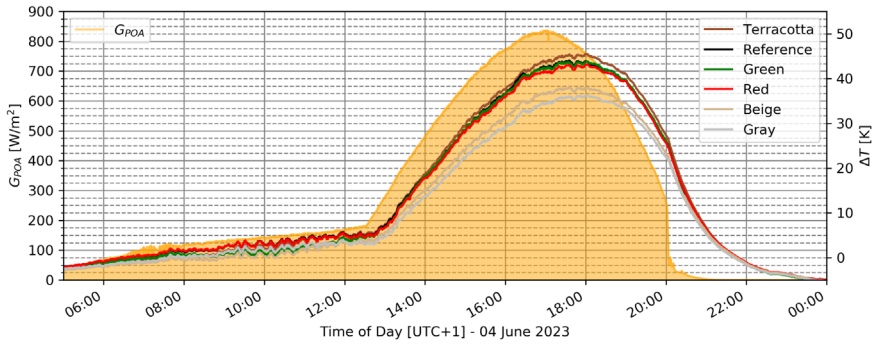

Fig. 3. Back-of module temperature difference to ambient for each module in the BIPV façade on a clear-sky day.

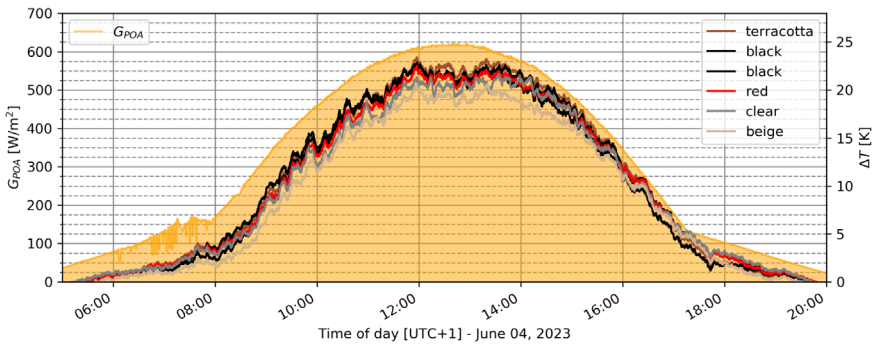

Fig. 4. Cell temperature difference to ambient for each coupon on a clear-sky day.

modules compared to the irradiance, caused by the large thermal mass of the glass-glass modules and the insulated mounting configuration. Additionally, the samples can be clearly separated into two groups, based on their temperature difference to ambient: While the terracotta-, green- and red-colored modules show similar temperatures to the reference, both the beige- and gray-colored modules are significantly cooler, in the maximum by more than 5 K.

Figure 4 shows a similar picture for the single-cell coupons, with the temperature difference comparing the measured cell temperature instead of the back-of-module temperature to the ambient. Due to the better ventilation, however, the thermal capacitance is less apparent and temperature differences are overall lower than in the façade mounted elements. Nevertheless, the beige-colored sample again shows a lower ΔT then all others.

A histogram of ΔT as a function of in-plane irradiance G_{POA} is shown in Figure 5, including linear fits for the Ross temperature coefficients k_{Ross}. Figure 6 shows the relative temperature differences ΔT_{rel} as function of irradiance. Similar to the Ross coefficients, a linear fit for each data series is included, albeit constrained to irradiances above 200 W/m^2 to exclude nighttime and cloudy conditions. The Ross coefficients and fitted ΔT_{rel} values at 1000 W/m^2 are shown in Table 1.

As can be expected from the earlier figures, the red-, green- and terracotta-colored modules all show similar Ross coefficients and relative temperature differences to the reference, showing constant fit-lines for the latter. The beige- and gray-colored modules, however show significantly lower Ross coefficients and relative temperature differences of approximately 10–30 %. The determined Ross coefficients correspond well to those reported in literature [5], and show that aside from mounting configuration, module coloration can play a significant factor. Of note is also the noticeable slope of the fit-lines, caused by a large cluster of higher temperature deviations at low irradiances.

Figure 7 and Table 2 show similar graphs and fitted values for the colored mini-modules, using the average temperature between the two black reference samples to calculate ΔT_{rel}. Compared to Figure 6, data points are much less spread out and only a small reduction (<10 %) in ΔT_{rel} can be observed for the beige-colored sample. While the fit-line shows no significant slope, the spread of temperature differences at low irradiances is noticeably bigger for the beige-colored sample than all others.

As of yet it is unknown why this slope can be observed in the façade but not in the single-cell coupons. A possible explanation could be consistent, rapid irradiance changes during sunset for the west-facing façade, which the south-facing mini-modules do not experience. Nevertheless, it seems clear that the color of the BIPV elements has an impact on the module temperature.

3.1 Relative transmittance

One of the most significant reductions to the effective irradiance seen by the PV cells is caused by absorption and reflection losses in the colored interlayers. Table 3 shows

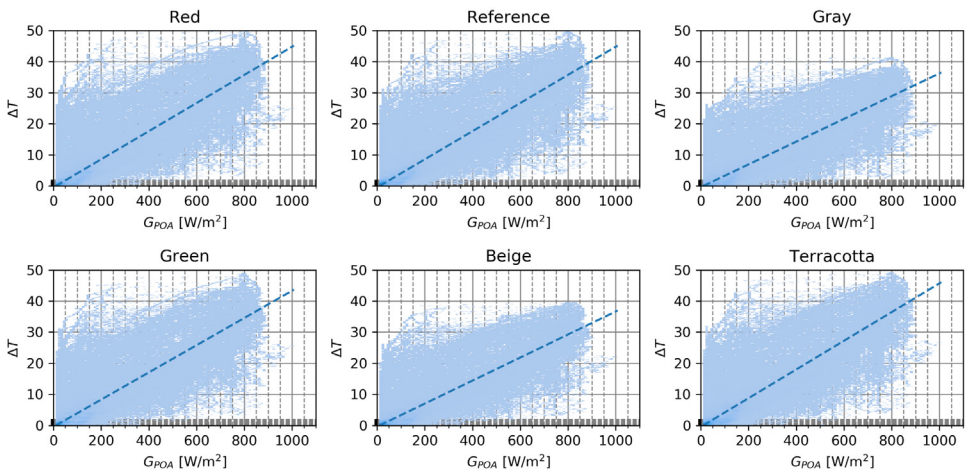

Fig. 5. Fitted Ross temperature coefficients for BIPV façade modules.

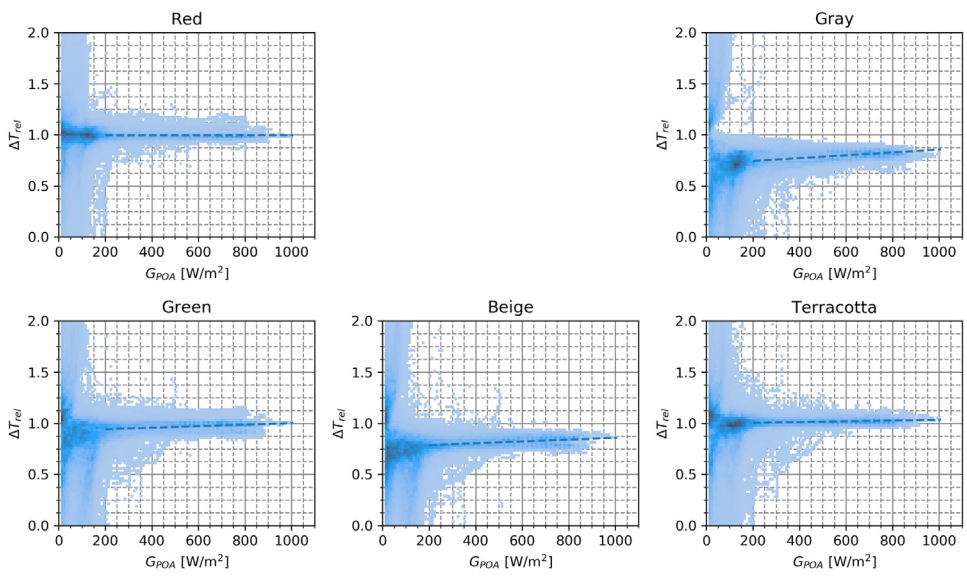

Fig. 6. Relative temperature difference compared to reference as a function of irradiance.

the relative transmittance under STC as obtained from the I_{sc} ratios in equation (2). This parameter can also be considered a measure for the relative module efficiency.

It can be clearly seen that there is no good correlation between transmittance and module temperature, as there is a significant loss of transmitted light even for samples showing similar temperatures to the reference. For example, the terracotta-colored samples show temperatures similar to or even higher than the reference samples without coloration, despite significant optical losses.

Furthermore, even though they show the lowest operating temperatures, neither the gray- nor the beige-colored sample have the lowest transmittance among the selected colors. Since sunlight absorbed in the colored interlayer is converted to heat without allowing for electricity generation, this leads to similar module temperatures for most colored modules compared to the reference.

3.2 Spectral reflectance

A more likely explanation for the lower temperature found in the gray- and beige-colored BIPV elements can be found in the total reflection spectra, as shown in Figure 8. For both of the light colors, a significantly higher reflectance can be observed over the entire spectral range compared to all other colors.

To allow for a better comparison to measurement data, the spectral reflectance $R(\lambda)$ is weighted by the AM1.5 spectrum and spectral response SR of the used cells and subsequently integrated, resulting in the weighted total reflectance R' according to equation (3). The results of this equation are shown in Table 4 as well as the relative effective irradiance G'_{rel}, when only taking reflection losses at normal incidence into account, calculated using equation (4). $R'(ref)$ here refers to the weighted total reflectance of the

Table 1. Fitted Ross coefficients and relative temperature differences at STC irradiance for BIPV façade modules.

Sample	Reference	Red	Gray	Green	Beige	Terracotta
k_{Ross} [Km^2/W]	0.0454	0.0452	0.0366	0.0438	0.0370	0.0462
ΔT_{rel} (@1000 W/m^2)	1	0.996	0.856	1.002	0.858	1.034

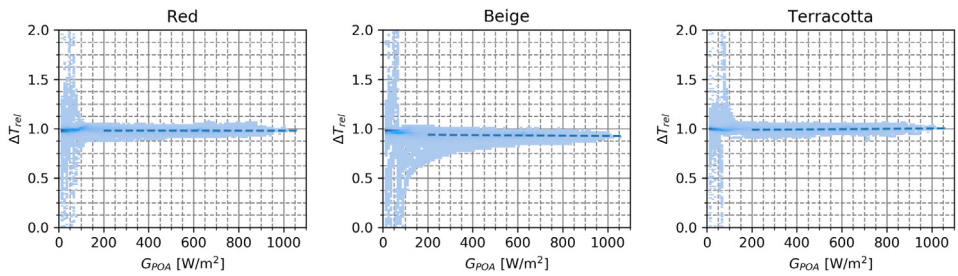

Fig. 7. Relative temperature difference compared to average of black references as a function of irradiance.

Table 2. Fitted relative temperature difference at STC irradiance for coupon samples.

Sample	Red	Beige	Terracotta
ΔT_{rel} (@1000 W/m^2)	0.979	0.927	1.002

Table 3. Relative transmittance in colored interlayers and fitted temperature differences (repeated from Tab. 1).

Sample	Reference	Red	Gray	Green	Beige	Terracotta
τ_{rel}	1	0.64	0.75	0.80	0.68	0.82
ΔT_{rel} (@1000 W/m^2)	1	0.996	0.856	1.002	0.858	1.034

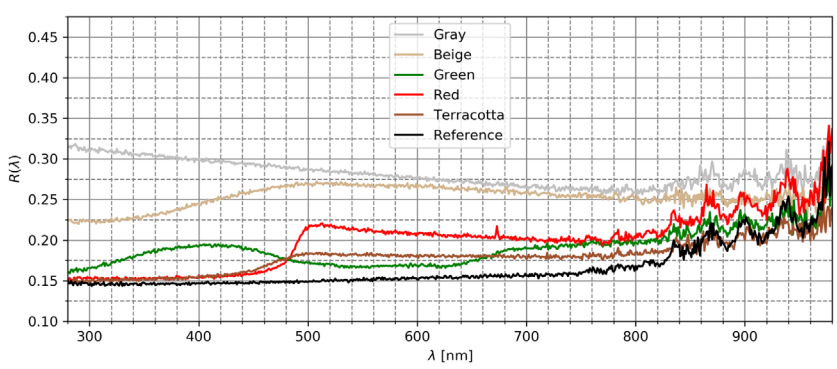

Fig. 8. Total spectral reflectance measured on PV modules.

Table 4. Weighted total reflectance, relative effective irradiance and fitted relative temperature differences (repeated from Tab. 1).

Sample	Reference	Red	Gray	Green	Beige	Terracotta
R'	0.16	0.20	0.28	0.19	0.25	0.18
G'_{rel}	1	0.96	0.86	0.97	0.90	0.98
ΔT_{rel} (@1000 W/m^2)	1	0.996	0.856	1.002	0.858	1.034

reference sample.

$$R' = \frac{\int R(\lambda) \cdot G_{AM1.5}(\lambda) \cdot SR(\lambda) d\lambda}{\int G_{AM1.5}(\lambda) \cdot SR(\lambda) d\lambda}, \quad (3)$$

$$G'_{rel} = \frac{1 - R'}{1 - R'(ref)}. \quad (4)$$

As can be seen in the table, G'_{rel} shows a significantly better correlation with the relative temperature differences, despite some deviations.

In case of the red-, green- and terracotta-colored samples, all three show comparable temperatures to the reference, while having a significantly higher reflectance. However, this deviation can most likely be explained by a larger part of the non-reflected light contributing to module heating, as all light absorbed in the colored interlayers is converted to heat.

For the gray- and beige-colored samples, this effect is also present, however due to the significantly higher total reflectance, this lower power conversion efficiency of non-reflected light cannot fully compensate for the reduced effective irradiance. In fact, since G'_{rel} is higher than ΔT_{rel}, it is likely that very little light is absorbed in the gray- and beige-colored interlayers at all.

4 Discussion

The results shown here have several implications both for modelling colored BIPV temperature and performance, as well as for designing new coloring technologies and products:

To improve temperature and performance models for colored BIPV, it is recommended to account for reflection losses separately from absorption losses. Instead of basing both temperature and PV performance on the same effective irradiance, temperature models should be based on the effective irradiance at the coloration layer, while performance models should continue to use the effective irradiance at the cell level. By considering absorption losses separately from reflection losses, their contribution to module heating can be more accurately captured. The currently common approach of basing temperature models mainly on the effective irradiance at cell level can lead to significant underestimation of module temperatures of pigment-based colored BIPV samples.

Regarding the design of coloring technologies relying on absorption, attention has to be paid to total reflectance as well as transmittance. If a choice has to be made between a more highly absorbing or more highly reflecting colorant (for similar total transmittance), the latter is to be preferred, as it can lead to significantly lower module temperatures. This however is less relevant for other coloring technologies, such as structural colors, which anyway have negligible absorption losses.

5 Conclusion

This work has shown the temperature difference caused by differently colored, pigment-based interlayers for BIPV modules. Significantly lower temperature for gray- and beige-colored samples were observed in an outdoor BIPV façade test stand as well as in single-cell mini-modules. In the west-facing BIPV façade, a noticeable change in relative temperature difference was observed for the gray- and beige-colored modules, however since the same effect could not be observed in the coupon setup, it is suspected to originate from rapid irradiance fluctuation caused by horizon shading around sunset.

It has been shown that there is poor correlation between the relative temperature difference observed and the measured total optical loss caused by the colored interlayers. Instead, good correlation was shown with the spectrally-weighted total reflectance, which indicates that absorption in the pigments significantly contributes to module heating. For modelling temperature in colored BIPV modules, it is therefore recommended to use an effective irradiance at the coloration layer – disregarding absorption losses – instead of at the cell, as is necessary for performance modelling.

Overall, this work has shown the need for further research and optimization of performance models specifically for colored BIPV, as the more complicated optical structure introduces significant error sources in the modelling process.

The authors would like to thank EUDP for financial support for the project Unit Sun under grant 64021-1079 as well as the project partners HS Hansen and MG Solar for their involvement in the construction of the test site.

Author contribution statement

M. Babin contributed to the construction and instrumentation of the façade test site and is responsible for the reflectance measurements, main data processing and analysis as well as writing of the manuscript. I.H. Jóhannsson is responsible for the coupon test stand and initial data analysis. M.L. Jakobsen provided input to optical measurements and calculations. S. Thorsteinsson contributed to construction and instrumentation of the test sites and is responsible for the overall project supervision. In addition, all authors were involved in reviewing and revising of the manuscript.

References

1. G. Peharz, A. Ulm, Renew. Energy **129**, 299 (2018)
2. J. Halme, P. Mäkinen, Energy Environ. Sci. **12**, 1274 (2019)
3. J.S. Stein, *Photovoltaic solar energy* (John Wiley & Sons, Ltd, 2016), pp. 564–578
4. E. Ozkalay, G. Friesen, M. Caccivio, P. Bonomo, A. Fairbrother, C. Ballif, A. Virtuani, IEEE J. Photovolt. **12**, 133 (2022)
5. N. Martín-Chivelet, J. Polo, C. Sanz-Saiz, L.T. Núñez Benítez, M. Alonso-Abella, J. Cuenca, Sustainability **14**, 1500 (2022)
6. D.L. King, J.A. Kratochvil, W.E. Boyson, Tech. Rep. SAND-97-1169C; CONF-970953-, Sandia National Lab. (SNL-NM), Albuquerque, NM (United States) (1997), https://www.osti.gov/biblio/548687
7. Y. Rao Golive, A. Kottantharayil, N. Shiradkar, Sol. Energy **237**, 203 (2022)
8. Z. Zhang, M. Wu, Y. Lu, C. Xu, L. Wang, Y. Hu, F. Zhang, Renew. Energy **155**, 658 (2020)
9. M. Babin, S. Thorsteinsson, A. Santamaria Lancia, P. Poulsen, A. Thorseth, C. Dam-Hansen, M. Jakobsen, Dependency of IAM losses in colored BIPV products on the refractive index of colorants, in *38th European Photovoltaic Solar Energy Conference and Exhibition*, 2021, pp. 583–588, https://doi.org/10.4229/EUPVSEC20212021-4BO.4.2
10. I.H. Jóhannsson, Master's thesis, (DTU, 2023), https://findit.dtu.dk/en/catalog/641a5551d4b5993c29f967aa

Cite this article as: Markus Babin, Ingvar Haukur Jóhannsson, Michael Linde Jakobsen, Sune Thorsteinsson, Experimental evaluation of the impact of pigment-based colored interlayers on the temperature of BIPV modules, EPJ Photovoltaics **14**, 34 (2023)